Resonant angular conversion in a Fabry–Perot resonator holding a dielectric cylinder

E. N. Bulgakov, A. F. Sadreev,* V. P. Gerasimov, and V. Y. Zyryanov

Kirensky Institute of Physics, Siberian Branch of Russian Academy of Sciences, Krasnoyarsk 660036, Russia
**Corresponding author: almas@tnp.krasn.ru*

Received October 30, 2013; accepted November 28, 2013;
posted December 12, 2013 (Doc. ID 200370); published January 13, 2014

Light transmission through a Fabry–Perot resonator (FPR) holding a dielectric cylinder rod is considered. For the cylinder parallel to mirrors of the FPR and the mirrors mimicked by the δ functions we present an exact analytical theory. It is shown that light transmits only for resonant incident angles, α_m, similar to the empty FPR. However after transmission the light scatters into different resonant angles, $\alpha_{m'}$, performing resonant angular conversion. We compare the theory with experiment in the FPR, exploring multilayer films as the mirrors and glass cylinder with diameter coincided with the distance between the FPR mirrors. The measured values of angular light conversion agree qualitatively with the theoretical results.

OCIS codes: (050.2230) Fabry-Perot; (260.2710) Inhomogeneous optical media; (050.1755) Computational electromagnetic methods.
http://dx.doi.org/10.1364/JOSAA.31.000264

1. INTRODUCTION

The Fabry–Perot resonator (FPR) is one of the most salient and simple manifestations of wave interference. If plane wave $\exp(ik_x x + ik_y y + ik_z z)$ is incident over a range of angles, the FPR transmits and reflects light into narrow bright fringes. This resonant transmission occurs for arbitrary fixed frequency $\omega = ck$, but for the discrete set of incident angles, α_m, defined by an equality [1]

$$\cos\,\alpha_m = \frac{m\lambda}{2d}, \tag{1}$$

where λ is the wavelength of the light, d is the length of the FPR cell, and m are the integers. It is important to note that the incident angle α is preserved for the light transmission through the FPR so there are no transitions between resonant incident angles, α_m, and transmitted angles, $\alpha_{m'}$, which is the result of space homogeneity in the directions parallel to the FPR mirrors.

However, if this homogeneity is violated, one can expect transitions between the incident resonant angles, α_m, into the different reflected and scattered angles, $\alpha_{m'}$, with $m \neq m'$. In the present paper we consider this phenomenon, inserting a single dielectric cylinder between the mirrors of the FPR. By mimicking the mirrors of the FPR by the δ functions we present an exact analytical theory for light transmission through such a filled FPR. We verify the theory by experimental measurements of the light intensity transmitted through the FPR holding a glass cylinder whose diameter equals the distance between the mirrors of FPR. The multilayer films are used as the mirrors of a good quality.

2. SCATTERING OF A CYLINDRICAL WAVE OF A SINGLE CYLINDER NEAR A SINGLE MIRROR

We start with the consideration of a single cylinder placed parallel to a single mirror, as shown in Fig. 1, where the z axis is directed along the cylinder. For the plane wave vector, $\vec{k}$, perpendicular to the z axis we can write the Maxwell equations in the form of a 2D Helmholtz equation [2],

$$\nabla^2\psi(x,y) + k^2\epsilon(x,y)\psi(x,y) = 0. \tag{2}$$

Here $\psi = E_z$ is the electric field directed along the z axis, the dielectric constant $\epsilon(x,y) = 1$ everywhere except the interior of the cylinder. The problem is close to plane-wave scattering by a cylinder parallel to a reflecting flat surface [3–5]. We mimic the mirror by the δ function, $\epsilon(x) = (\mu/k^2)\delta(x)$. The factor μ defines the coupling between two half spaces, i.e., the quality of the mirror. Then the boundary conditions take the following form [6]:

$$\psi(-0,y) = \psi(+0,y), \quad \frac{\partial\psi(-0,y)}{\partial x} - \frac{\partial\psi(+0,y)}{\partial x} = \mu\psi(0,y). \tag{3}$$

We show that these boundary conditions are satisfied by introduction of a fictitious source (FS) symmetrically placed relative to the mirror as shown in Fig. 1 by the yellow circle (on the right), although the FS is a point.

The cylinder scatters the plane wave into the superposition of the outgoing cylindrical waves given by the Hankel functions of the first order [2,4],

$$\psi^{(\mathrm{cyl})}(r,\phi) = \sum_m b_m^{(s)} H_m^{(1)}(kr)\exp(im\phi), \tag{4}$$

where

$$b_m^{(s)} = i^m S_m = \frac{qJ'_m(kR)J_m(qR) - J_m(kR)J'_m(qR)}{H_m(kR)J'_m(qR) - qH'_m(kR)J_m(qR)}, \tag{5}$$

and $q = \sqrt{\epsilon}k$. In turn, each mth cylindrical wave undergoes reflection and transmission through the mirror. We try the transmitted wave at $x \geq 0$, in the form

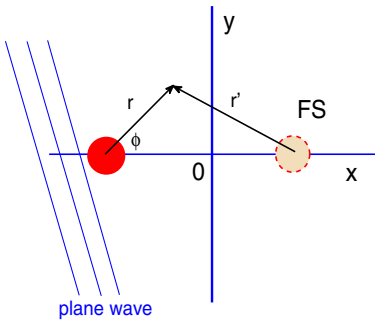

Fig. 1. Single dielectric cylinder shown by red (left circle) and its fictitious image (yellow, right circle) spaced symmetrically relative to the single mirror.

$$\psi^{(t)}(r,\phi) = \sum_n b_n^{(t)} H_n^{(1)}(kr)\exp(in\phi), \tag{6}$$

and the reflected wave at $x \le 0$ as

$$\psi^{(r)}(r',\phi) = \sum_n b_n^{(r)} H_n(kr')\exp[in(\pi-\phi)], \tag{7}$$

where $r' = |\vec{r} - 2h\vec{e}_x|$ is the radius referred to the FS, as shown in Fig. 1. Obviously, both trial functions obey Eq. (2) and the boundary conditions at the surface of the dielectric cylinder. In order to satisfy the boundary conditions at the mirror's surface we substitute the trial functions (6) and (7) into Eq. (3) and determine that the reflected amplitudes are linked with the transmitted amplitudes as follows:

$$b_n^{(t)} = \sum_m F_{n-m} b_m^{(s)}, \qquad b_n^{(r)} = -b_n^{(s)} + b_n^{(t)} \tag{8}$$

with $F_m = F_m^{(1)} + F_m^{(2)}$, where

$$F_m^{(1)} = \begin{cases} -\frac{\gamma}{1+\gamma(q_2-q_1)} q_1^{m+1}, & m \ge -1, \\ -\frac{\gamma}{1+\gamma(q_2-q_1)} q_2^{-m-1}, & m \le -1, \end{cases} \tag{9}$$

$$F_m^{(2)} = \begin{cases} \frac{\gamma}{1+\gamma(q_2-q_1)} q_1^{m+1}, & m \ge 1, \\ \frac{\gamma}{1+\gamma(q_2-q_1)} q_2^{-m-1}, & m \le 1, \end{cases} \tag{10}$$

$$q_1 = \frac{1-\sqrt{1+4\gamma^2}}{2\gamma}, \qquad q_2 = \frac{2\gamma}{1+\sqrt{1+4\gamma^2}}, \tag{11}$$

$\gamma = k/\mu$. Equation (8) shows that the cylindrical wave with the amplitude $b_m^{(s)}$ for transmission through the δ function plane mirror undergoes a simple linear transformation, with the transfer matrix, $\hat{F}$. That result is exact and presents substantial simplification compared to Refs. [3–5] for a cylinder buried in a dielectric slab.

3. FPR WITH SINGLE DIELECTRIC CYLINDER

In this section we develop the approach of expansion over cylindrical waves for the case of two parallel δ function mirrors and a single infinite dielectric cylinder placed symmetrically between and parallel to mirrors, as shown in Fig. 2. This

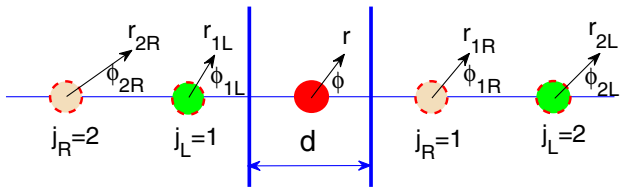

Fig. 2. Single dielectric cylinder shown by the red circle (above the d) is spaced between two parallel mirrors (a view from above). The cylinder is parallel to the mirrors. The first sequence of FSs, shown by yellow and labeled by the index j_R, begins after the reflection of the actual cylinder at the right mirror to produce the $j_R = 1$ FS, then it reflects at the left mirror to produce the $j_R = 2$ FS, etc. The second set of FSs, shown by green and labeled by the index j_L, begins after the reflection at the left mirror.

assumption reduces the 3D problem of light transmission to the 2D one similar to the previous section.

We start with the solution inside of the empty FPR,

$$[A\exp(ik_x x) + B\exp(-ik_x x)]\exp(ik_y y), \quad -d/2 < x < d/2. \tag{12}$$

The problem is equivalent to the one-dimensional problem of transmission of quantum particle through two δ function potentials [7]. As a result, we obtain

$$A = 1 + \frac{i\mu}{2k_x} + \frac{\mu^2}{2k_x^2}\frac{\cos k_x d + \frac{\mu}{2k_x}\sin k_x d}{\left(1+\frac{i\mu}{k_x}\right)e^{-ik_x d} + \frac{\mu^2}{k_x^2}(e^{ik_x d} - e^{-ik_x d})},$$

$$B = -\frac{i\mu}{2k_x} - \left(1 - \frac{i\mu}{2k_x}\right)\frac{i\mu}{2k_x}\frac{\cos k_x d + \frac{\mu}{2k_x}\sin k_x d}{\left(1+\frac{i\mu}{k_x}\right)e^{-ik_x d} + \frac{\mu^2}{k_x^2}(e^{ik_x d} - e^{-ik_x d})}. \tag{13}$$

To consider the scattering of the solution [Eq. (12)] by the cylinder we expand it over the cylindrical waves

$$\psi_{\text{empty}}(r,\phi) = \sum_m i^m J_m(kr)[Ae^{im(\phi-\alpha)} + (-1)^m Be^{im(\phi+\alpha)}] = \sum_m a_m^{(0)} J_m(kr)e^{im\phi}, \tag{14}$$

where α is the incident angle. Each cylindrical wave in Eq. (14) undergoes the same processes of scattering by each mirror as were considered explicitly in the previous section by introducing the FS. However, in the case of two mirrors, the actual cylinder gives rise to multiple FSs, shown by the yellow and green, which results in the multiple scattering of cylindrical waves by two parallel mirrors. Following Ref. [2], we consider the fields scattered by all FSs (yellow in Fig. 2) toward the actual cylinder (red), which act on this cylinder as incident fields. These fields complemented to the incident plane waves [Eq. (14)] constitute the total incident field relative to the actual cylinder,

$$\psi_{\text{inc}}(r,\phi) = \psi_{\text{empty}}(r,\phi) + \psi_{\text{fict}}(r,\phi) = \sum_m (a_m^{(0)} + a_m^{(\text{fict})}) J_m(kr)e^{im\phi} = \sum_m a_m^{(\text{tot})} J_m(kr)e^{im\phi}, \tag{15}$$

which gives rise to scattering by the actual cylinder, similar to Eq. (4),

$$\psi_{\mathrm{scat}}(r,\phi)=\sum_m b_m^{(\mathrm{tot})}H_m^{(1)}(kr)e^{im\phi}, \tag{16}$$

where scattered, $b_m^{(\mathrm{tot})}$, and the incident, $a_m^{(\mathrm{tot})}$, amplitudes are linked via the diagonal scattering matrix [Eq. (5)]: $b_m^{(\mathrm{tot})}=S_m a_m^{(\mathrm{tot})}$ [2].

Therefore, the current problem is to calculate the effect of all FSs given by $a_m^{(\mathrm{fict})}$ that can be solved by the consequent application of the transformation [Eq. (8)]. In what follows, the letters a, b will refer to the ingoing and outgoing cylindrical waves [2]. In particular, the wave outgoing from the $j_R=1$ FS will be written as follows:

$$\psi^{(1)}(r_{1R},\phi_{1R})=\sum_n b_n^{(1)}H_n^{(1)}(kr_{1R})\exp(in\phi_{1R}), \tag{17}$$

with the amplitudes

$$b_n^{(1)}=\sum_m D_{n-m}b_m^{(\mathrm{tot})}, \tag{18}$$

where $D_n=F_n-\delta_{n,0}$. The upper index (1) specifies not only the first act of reflection at the right mirror but also the first right FS $j_R=1$, shown by yellow in Fig. 2.

Second, each cylindrical wave with the amplitude $b_n^{(1)}$ in Eq. (17) undergoes reflection at the left δ function mirror by the same transformation rules [Eq. (18)] established above. The difference is that the FS is positioned at the left, labeled in Fig. 2 by the index $j_R=2$. Therefore, the second reflected wave can be written as

$$\psi^{(2)}(r_{2R},\phi_{2R})=\sum_n b_n^{(2)}H_n^{(1)}(kr_{2R})\exp(in\phi_{2R}), \tag{19}$$

where arguments r_2, ϕ_2 refer to the centrum of the second FS $j_R=2$, and

$$b_n^{(2)}=\sum_m D_{n-m}b_m^{(1)}=\sum_m(\hat{D}^2)_{n-m}b_m^{(\mathrm{tot})}. \tag{20}$$

Therefore, we obtain a geometric series of cylindrical waves with FSs positioned at the sites j_R,

$$\psi=\sum_n\sum_{j_R=1}^{\infty}\sum_m(\hat{D}^k)_{n-m}b_m^{(\mathrm{tot})}H_n^{(1)}(kr_{j_R})\times\exp[in(\pi j_R+(-1)^{j_R}\phi_{j_R})]. \tag{21}$$

However, in accordance with Eq. (15). references of each FS are to be transferred to the centrum of the actual cylinder in order to obtain a closed system for amplitudes $b_m^{(\mathrm{tot})}$. That is performed by the use of the Graf formula [2]:

$$H_n^{(1)}(kr_{j_R})e^{in\phi_{j_R}}=\sum_m e^{i\pi(n-m)(j_R+1)}H_{m-n}^{(1)}(j_R kd)J_m(kr)e^{im\phi}, \tag{22}$$

where $j_R d$ are the distances between center of the actual cylinder and centers of the FSs.

We can write the following algebraic system of equations in accordance to Eq. (15),

$$a_m=a_m^{(0)}+\sum_n\hat{G}_{m-n}b_n^{(\mathrm{tot})}, \tag{23}$$

where the amplitudes, $a_m^{(0)}$, were defined in Eq. (14). Then, according to Eqs. (21) and (22), we obtain

$$G_m^{(R)}=\sum_{j_R}\sum_n(-1)^{j_R}H_{m-n}^{(1)}(j_R kd)(\hat{D}^k)_n. \tag{24}$$

A similar expression, $G_m^{(L)}$, can be obtained for the second series of FSs labeled by j_L (green in Fig. 2), where the radii, r_{j_L}, in Eq. (21) refer to the FS.

Finally, expressing each amplitude, $b_m=S_{mm}a_m$, we obtain the self-consistent system of linear algebraic equations for the amplitudes $b_m m^{(\mathrm{tot})}$,

$$b_m^{(\mathrm{tot})}=S_m a_m^{(0)}+\sum_n(G_{m-n}^{(R)}+G_{m-n}^{(L)})b_n^{(\mathrm{tot})}, \tag{25}$$

where the amplitudes, $a_m^{(0)}$, are given by Eq. (14). Formally, this set of equations is infinite. However, the matrix, $G_{m-n}^{L,R}$, is decayed with growth of $|n-m|$. The field transmitted through the FPR holding single dielectric cylinder is given by the contribution of all FSs at the left of the FPR plus the actual cylinder and can be written as follows

$$\psi_{VP}=\sum_j\sum_{mn}(\hat{F}\hat{D}^j)_{m-n}b_n^{(\mathrm{tot})}H_m^{(1)}(qR_j)e^{im\phi_j}, \tag{26}$$

where j runs over all FSs at the left including the actual cylinder. The matrix, $\hat{D}$, is defined by Eq. (20), R_j is the distance between the jth FS and the view point. In order to calculate $b_n^{(\mathrm{tot})}$ using Eq. (25) numerically, one hundred left FSs and one hundred right FSs were considered. That allowed the calculation of the intensity, $|\psi_{VP}|^2$, at the plane screen directed parallel to the FPR that is shown in Fig. 4.

4. EXPERIMENTAL REALIZATION

The layout of the FPR is shown in Fig. 3(a). The mirrors of the FPR are fabricated from multilayer films [8] comprised of 6 layers of zirconium dioxide (ZrO_2) with the refractive index 2.04 and thickness 52 nm, and 5 layers of silicon dioxide (SiO_2) with the refractive index 1.45 and thickness 102 nm, in alternating sequence. The layers are deposited on a fused quartz substrate. Normally-incident transmission spectra of the single dielectric mirror shows photonic band gap in the wavelength scale from 425 to 620 nm, as shown in Fig. 3(b) by a dashed line. The FPR holds a glass cylinder with the refractive index 1.55. The transmission spectra of the empty FPR, measured with a Shimadzu UV-3600 spectrophotometer, is presented in Fig. 3(b) by a solid line, for the light incident normally to the FPR.

A laser beam with the wavelength 532 nm, polarized parallel to the glass cylinder z axis, incidents on the FPR cell at the angle α_m to the x axis in the $x0y$ plane, as shown in Fig. 3(a). Respectively, the $y0z$ plane is parallel to the substrates. The glass cylinder is oriented along z axis and arranged in the center of the laser beam. We have chosen the minimal resonant incident angle, α_{26}. The angular distribution of

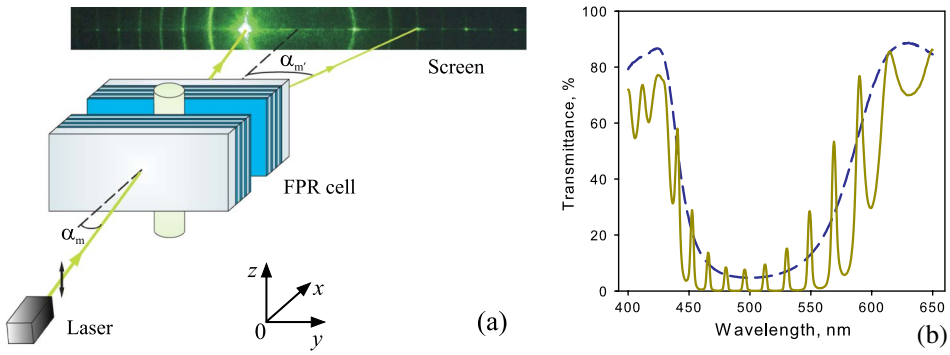

Fig. 3. (a) Optical setup of a laser beam transmission through the FPR holding the dielectric cylinder and (b) transmission spectra of single mirror (dash line) and double mirrors (solid line) for green light, $\lambda = 532$ nm.

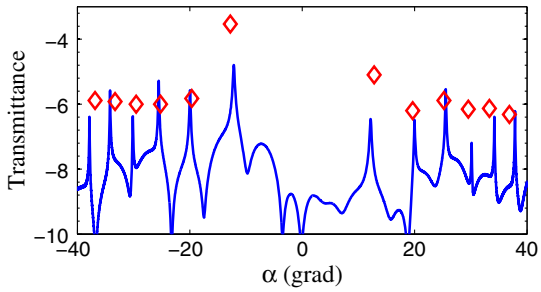

Fig. 4. Transmittance versus scattering angles of the light beams, for $d = 7.09$ μm. The solid line shows the intensity, $|\psi_{VP}|^2$, normalized by the input intensity in a log scale, calculated by use of Eq. (26), while diamonds show the experimental light transmittance in a log scale, measured for the resonant angles [Eq. (1)].

transmitted light scattering through the FPR cell is observed at a screen that is parallel to the cell. A photo of fringes of transmitted light behind the FPR cell is shown in Fig. 3, which reveals a distinct discrete structure. There is a set of discrete angles, $\alpha_{m'}$ defined by Eq. (1) at which the transmitted light goes out from the FPR. However, for the present experimental realization of the FPR with rather thick mirrors comparable with the light wavelength, it is unambiguous to define the distance d between the mirrors. Experimental values of the resonant peaks for the resonant angles are marked in Fig. 4 by diamonds, for $d = 7.09$ μm. The positions of the light spots are symmetric with respect to the normal to the FPR cell. A pinhole of a photodiode, which detects transmitted light, was chosen to be equal to the cross section of the laser beam. The measured transmittances in a log scale are compared in Fig. 4 to the theoretical results (solid curves) based on Eq. (26).

5. SUMMARY AND DISCUSSION

The dielectric cylinder gives rise to the scattering of a laser beam with angular distribution of the light intensity $|\psi^{(\mathrm{cyl})}(r,\phi)|^2$ given by Eqs. (4) and (5), which has no sharp angular behavior. We have shown, however, that if a cylinder is placed inside the FPR cell the angular distribution acquires exclusively sharp behavior. Our interpretation is based on an optical analogy with a diffraction lattice. As one can see from Fig. 2, the dielectric cylinder forms a regular lattice of FSs that can be presented as the 1D lattice of sources with the lattice unit equal to the distance between mirrors, similar to grating surfaces. Scattering of electromagnetic waves from such a grating leads to sharp angular behavior of scattered waves. Fig. 4 shows good quantitative agreement for the resonant angles, α_m, given by Eq. (1) and the qualitative agreement for resonant peaks in the transmittance. The reason for discrepancy in the transmittance, we speculate, is that the theory explores the delta function approximation for the FPR mirrors. In the experimental setup shown in Fig. 3 one can see that the mirrors are fabricated of the multilayered heterostructure; thereby the simple picture of FSs presented in Fig. 2 vanishes. Nevertheless, the presented theory qualitatively explains the resonant angular scattering for the light transmission through the FPR holding dielectric cylinder.

ACKNOWLEDGMENTS

This work was partially supported by RFBR grant 13-02-00497, and grants no. 43, 101 and 24.29 of SB RAS, and NSCT-SB RAS. We thank D. N. Maksimov for critical reading of the manuscript.

REFERENCES

1. M. Born and E. Wolf, *Principles of Optics: Electromagnetic Theory of Propagation, Interference and Diffraction of Light* (Cambridge University, 1999).
2. D. Maystre, S. Enoch, and G. Tayeb, "Scattering matrix method applied to photonic crystals," in *Electromagnetic Theory and Applications for Photonic Crystals*, K. Yasumoto, ed. (Taylor & Francis, 2006).
3. R. Borghi, M. Santarsiero, F. Frezza, and G. Schettini, "Plane-wave scattering by a dielectric circular cylinder parallel to a general reflecting flat surface," J. Opt. Soc. Am. A **14**, 1500–1504 (1997).
4. D. E. Lawrence and K. Sarabandi, "Electromagnetic scattering from a dielectric cylinder buried beneath a slightly rough surface," IEEE Trans. Antennas Propag. **50**, 1368–1376 (2002).
5. S.-C. Lee, "Scattering by a radially stratified infinite cylinder buried in an absorbing half-space," J. Opt. Soc. Am. A **30**, 565–572 (2013).
6. S. Flügge, *Practical Quantum Mechanics I* (Springer-Verlag, 1971).
7. P. Markoš and C. M. Soukoulis, *Wave Propagation From Electrons to Photonic Crystals and Left-Handed Materials* (Princeton University, 2008).
8. V. G. Arkhipkin, V. A. Gunyakov, S. A. Myslivets, V. Y. Zyryanov, and V. F. Shabanov, "Angular tuning of defect modes spectrum in the one-dimensional photonic crystal with liquid-crystal layer," Eur. Phys. J. E **24**, 297–302 (2007).